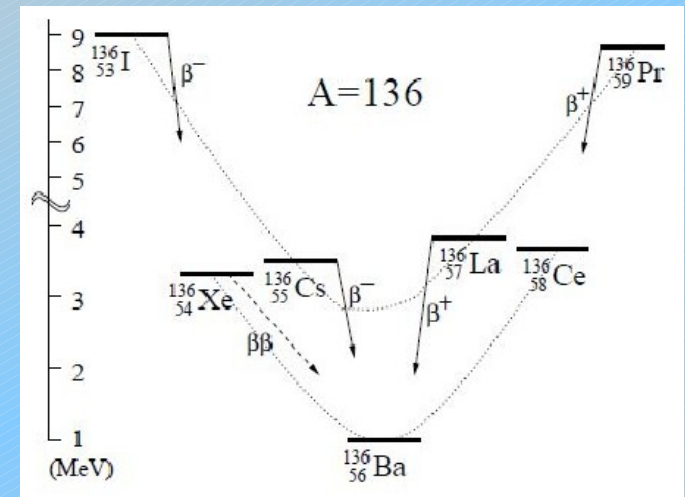
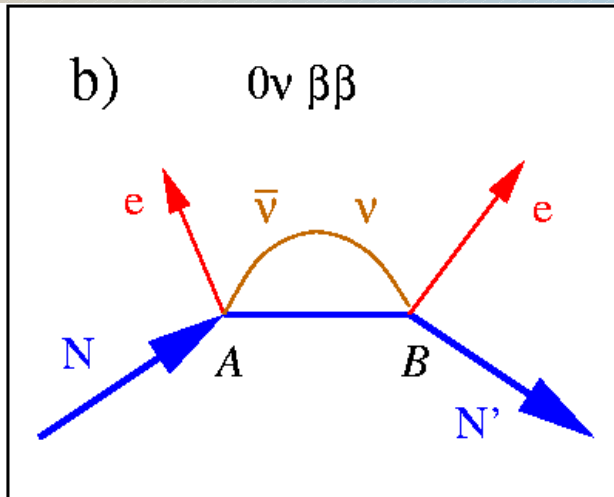
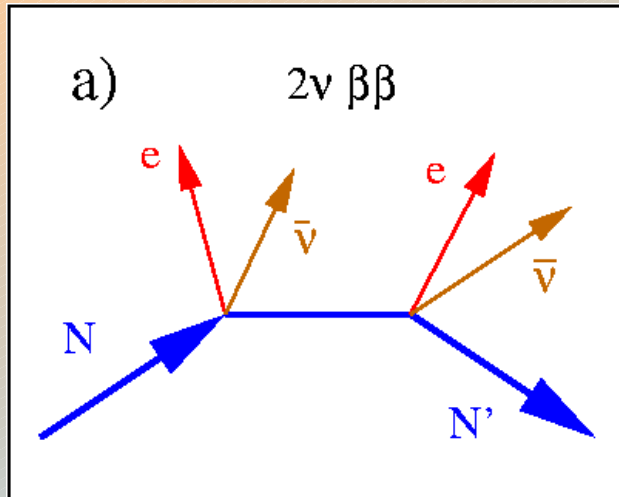


Recent results from EXO-200

Vladimir Belov, ITEP & MEPhI
for the EXO collaboration

16th Lomonosov Conference, Moscow, 23 August 2013

Double beta decay



2ν mode:

a conventional
2nd order process
in Standard Model

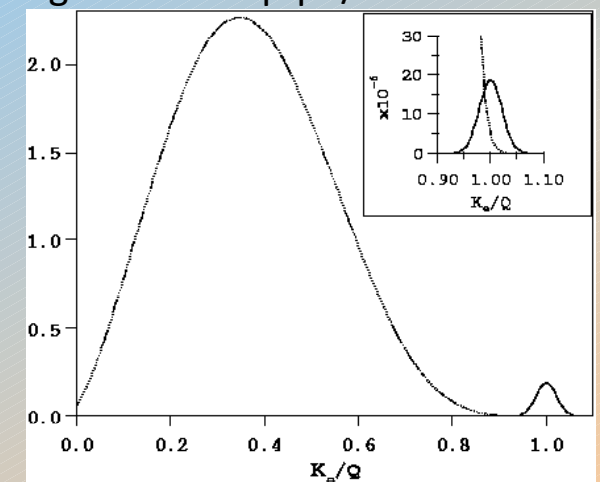
0ν mode:

a hypothetical process
can happen only if:
 $\langle m_\nu \rangle \neq 0, \nu = \bar{\nu}$
 $|\Delta L| = 2, |\Delta(B-L)| = 2$

To reach high measurement sensitivity for 0ν mode one requires,

- High energy resolution
- Large Isotope mass
- Low background

Simulated double beta decay spectrum
P.Vogel. arXiv:hep-ph/0611243



Why xenon

Energy resolution is poorer than the crystalline devices (~factor 10), but...

Monolithic detector. Xenon can form detection medium, allow self shielding, surface contamination minimized. Very good for large scale detectors.

Has high Q value. Located in a region relatively free from natural radioactivity.

Isotopic enrichment is easier. Xe is already a gas & ^{136}Xe is the heaviest isotope.

Xenon is “reusable”. Can be purified & recycled into new detector (no crystal growth).

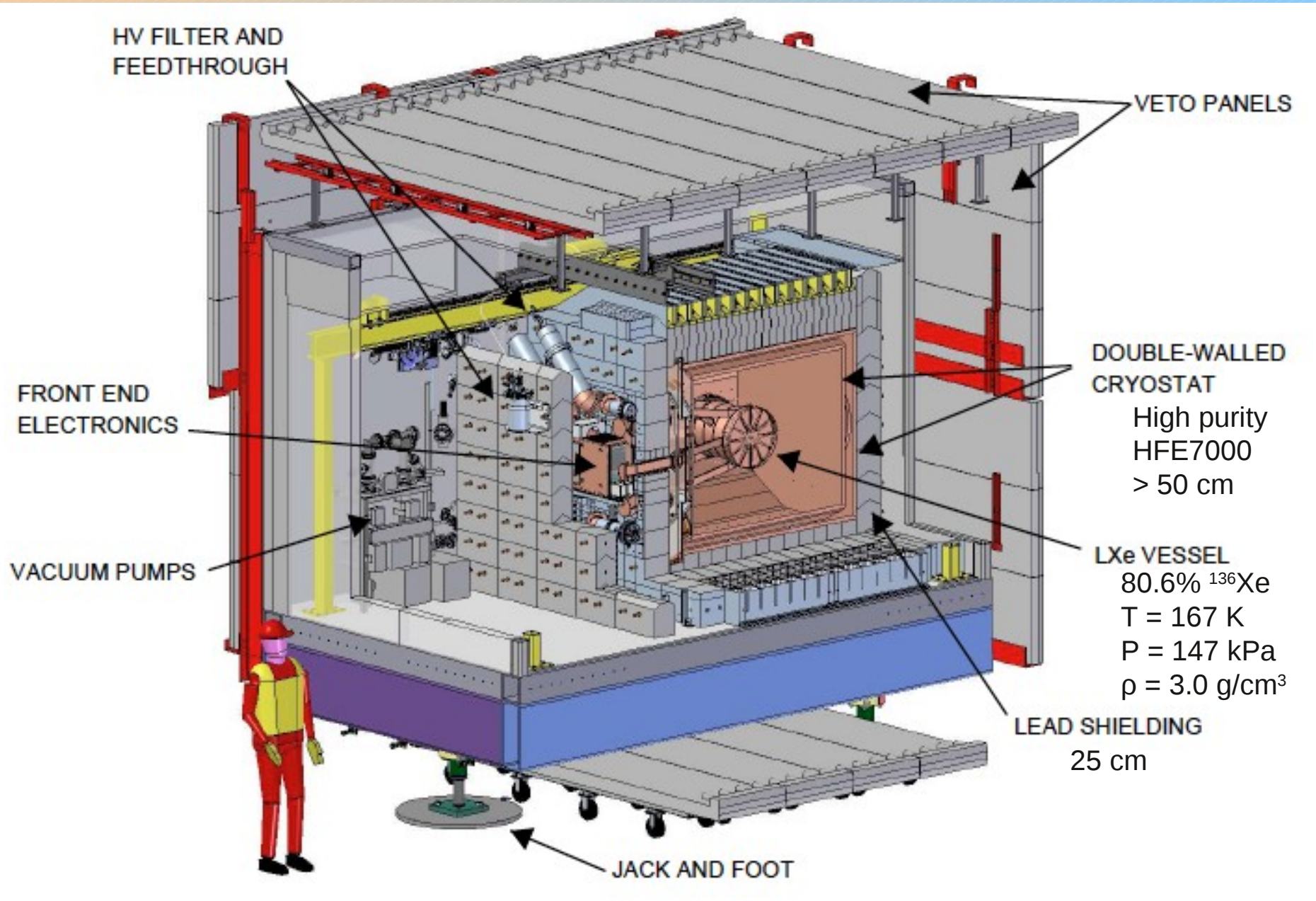
Minimal cosmogenic activation. No long lived radioactive isotopes of Xe.

Energy resolution in LXe can be improved. Scintillation light/ionization correlation.

Particle identification. Slightly limited, but can be used to tag alphas from Rn chain.

... admits a novel coincidence technique. Background reduction by Ba daughter tagging.

EXO-200 detector



The EXO-200 TPC

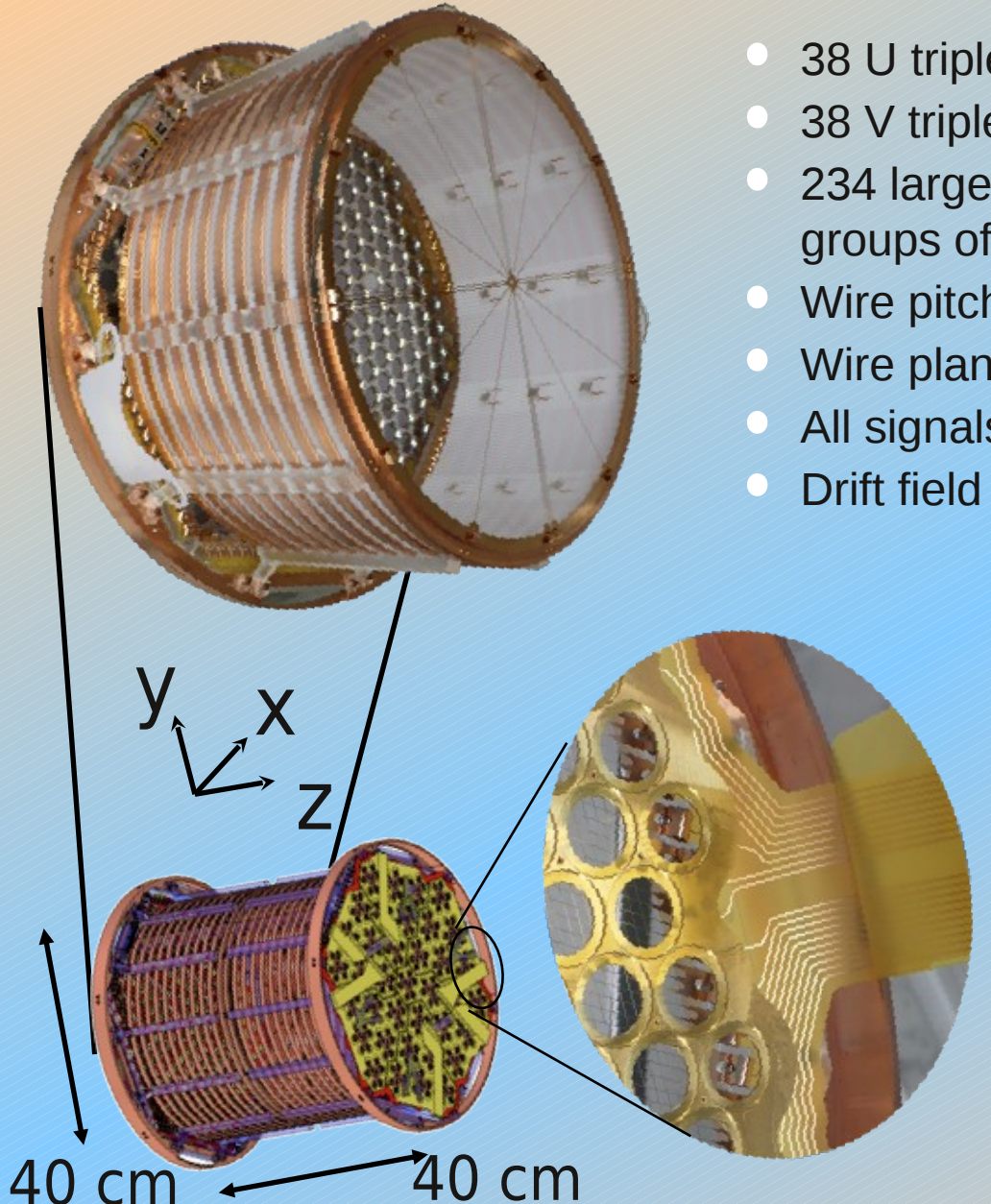
Two almost identical halves reading **ionization** and 178 nm **scintillation**, each with:

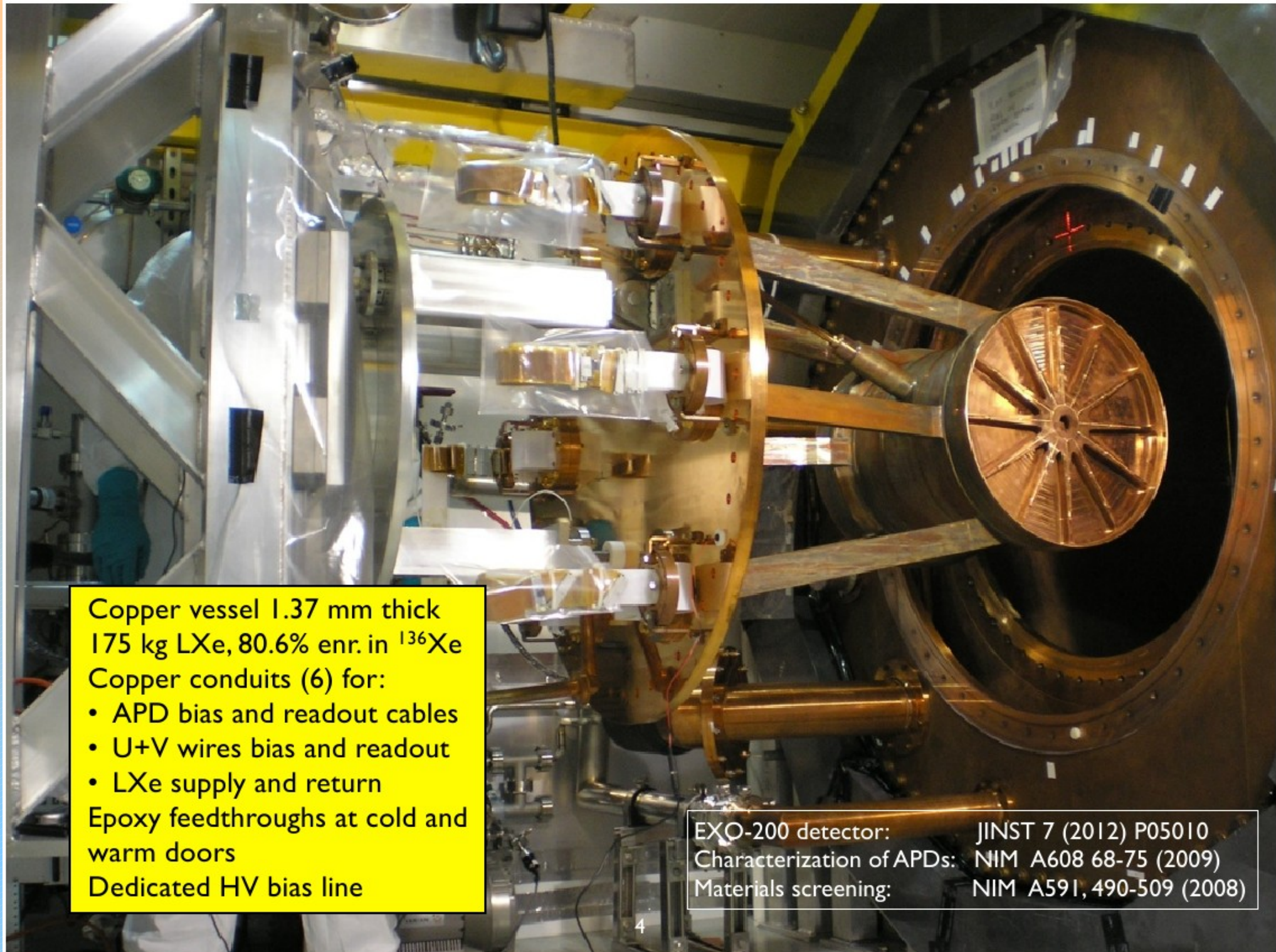
- 38 U triplet wire channels (charge)
- 38 V triplet wire channels, crossed at 60° (induction)
- 234 large area avalanche photodiodes (APDs, light in groups of 7)
- Wire pitch 3 mm (9 mm per channel)
- Wire planes 6 mm apart and 6 mm from APD plane
- All signals digitized at 1 MS/s, ±1024S around trigger
- Drift field 376 V/cm

- Field shaping rings: copper
- Supports: acrylic
- Light reflectors/diffusers: Teflon
- APD support plane: copper; Au (Al) coated for contact (light reflection)
- Central cathode, U+V wires: photo-etched phosphor bronze
- Flex cables for bias/readout: copper on kapton, no glue

Comprehensive material screening program

Goal: 40 cnts/2y in $0\nu\beta\beta \pm 2\sigma$ ROI, 140 kg LXe





Muon veto

50 mm thick plastic scintillator panels surrounding TPC on four sides.

$95.5 \pm 0.6\%$ efficiency

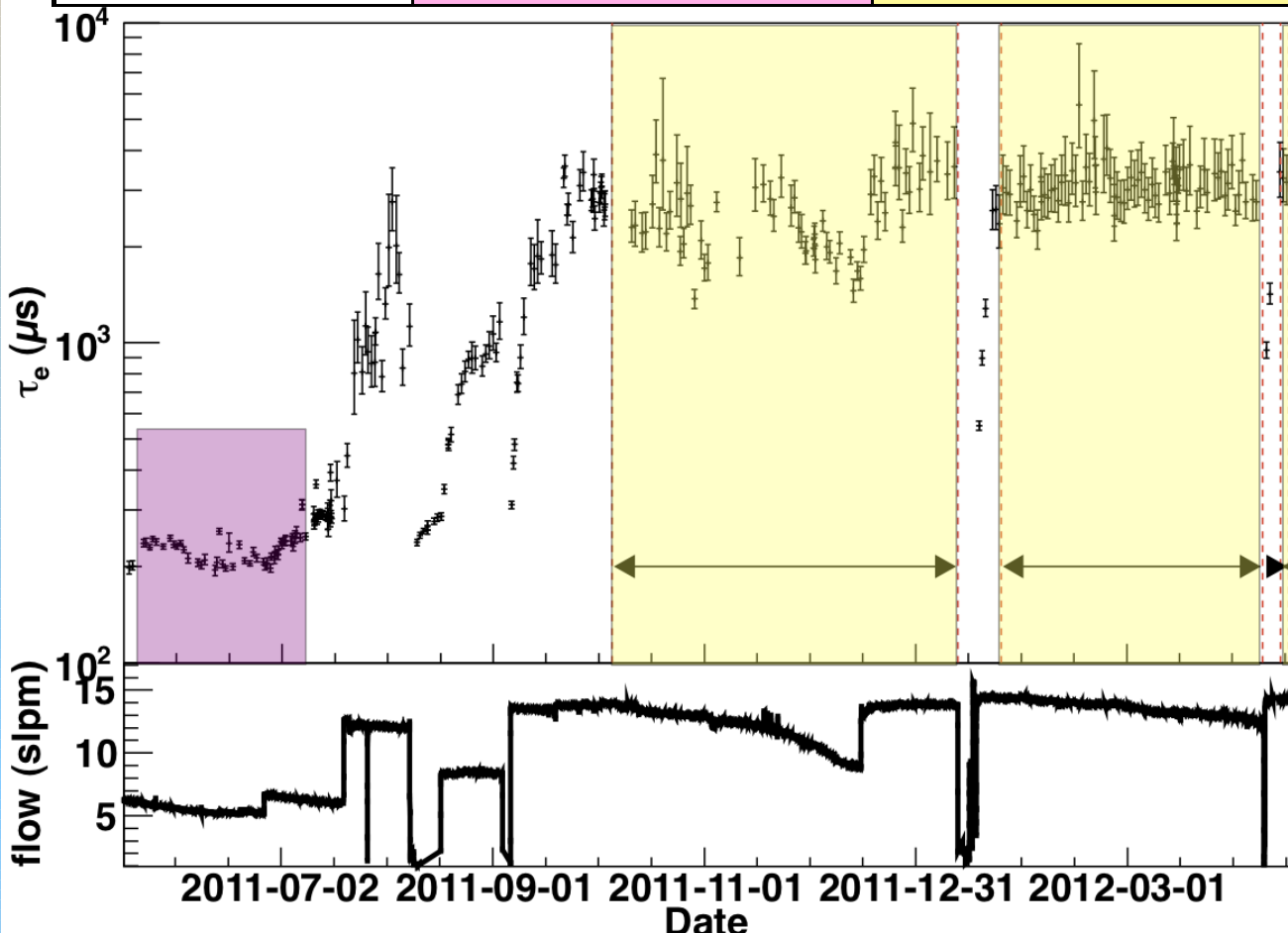
Veto cuts (8.6% combined dead time)

- 25 ms after muon veto hit
- 60 s after muon track in TPC
- 1 s after every TPC event



Data taking phases and xenon purity

	Run I	Run 2a
Period	May 21, 11 – Jul 9, 11	Sep 22, 11 – Apr 15,12
Live Time	752.7 hr	2,896.6 hr
^{136}Xe exposure	3.7 kg-yr	32.5 kg-yr
Publication	PRL 107 (2011) 212501	arXiv:1205:5608



Sep 2011 – Hardware upgrades
 •APD gain increase by factor 2
 •improved U-wire shaping
 •added outer lead shield

Purity

Electron lifetime τ_e is determined by measuring the attenuation of the ionization signal as a function of drift time for the full-absorption peak of gamma ray sources

For this analysis, the recirculation rate was increased to 14 slpm, leading to long electron lifetimes in the TPC

At $\tau_e = 3$ ms:
 •max. drift time $\sim 110 \mu\text{s}$
 •loss of charge is 3.6% at full drift length

Ultraclean pump:
 Rev Sci Instrum. 82(10):105114
 Xenon purity with mass spectroscopy:
 NIM A675 (2012) 40-46
 Gas purity monitors:
 NIM A659 (2011) 215-228

Event reconstruction

- Signal finding – matched filters applied on U,V and APDs waveforms
- Signal parameter estimation (t , E) for charge and light
- Cluster finding – assignment to Single Site (SS) or Multiple Site (MS): resolution 18mm in X and Y and 6 mm in Z

Amplitudes corrected by channel for gain variation

Signal fitting functions use individual parameters for each channel

Optimized light correction using charge position

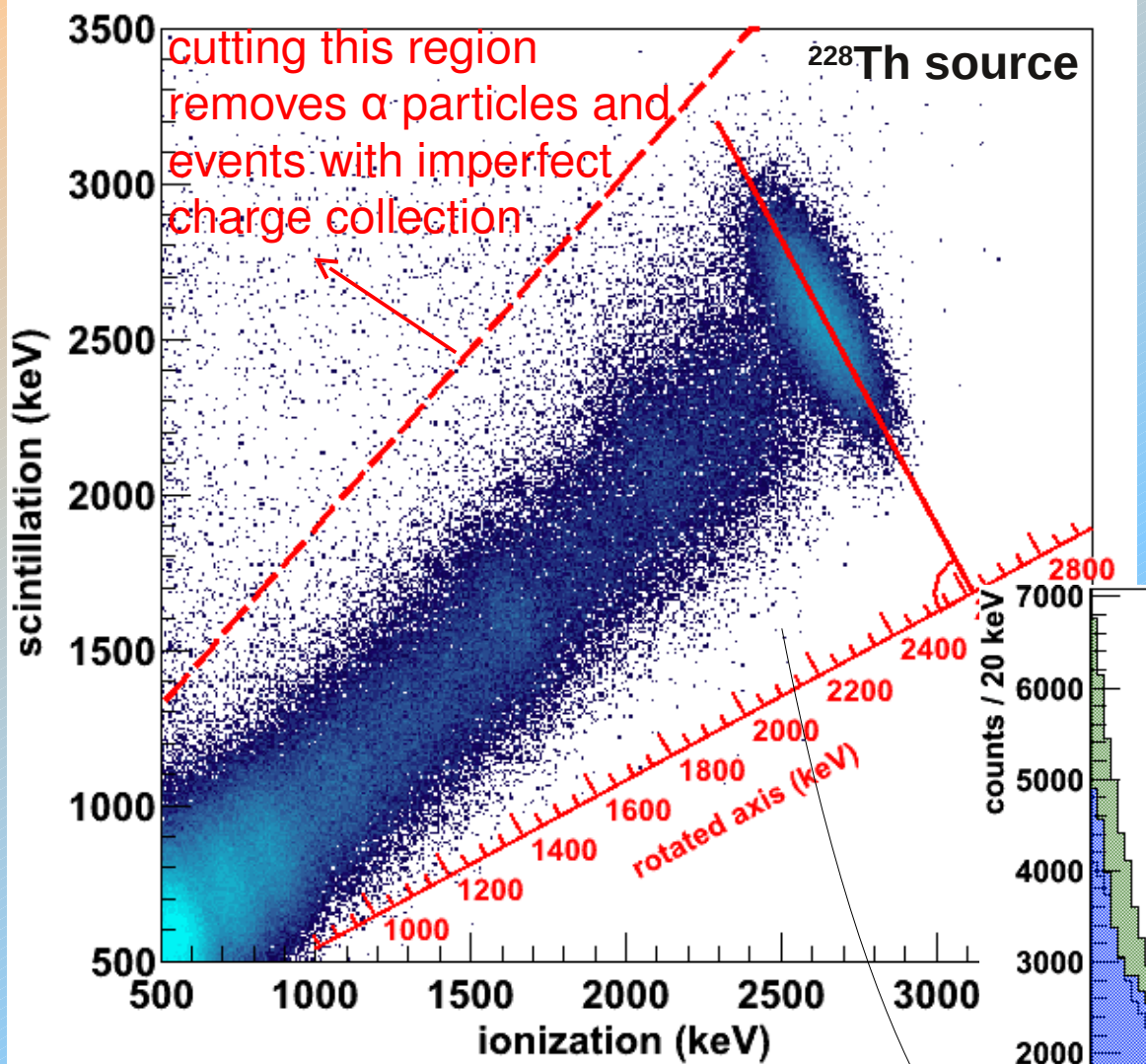
Charge corrected for inefficiency on small drift

Require events to be fully reconstructed in 3D

Reconstruction efficiency for $0\nu\beta\beta$ is 71% – estimated by MC and verified by comparing the $2\nu\beta\beta$ MC efficiency with low background data, over a broad range in energy

SS and MS spectra are fitted simultaneously with MC-generated probability density functions

Combining ionization and scintillation



Rotation angle chosen to optimize energy resolution at 2615 keV

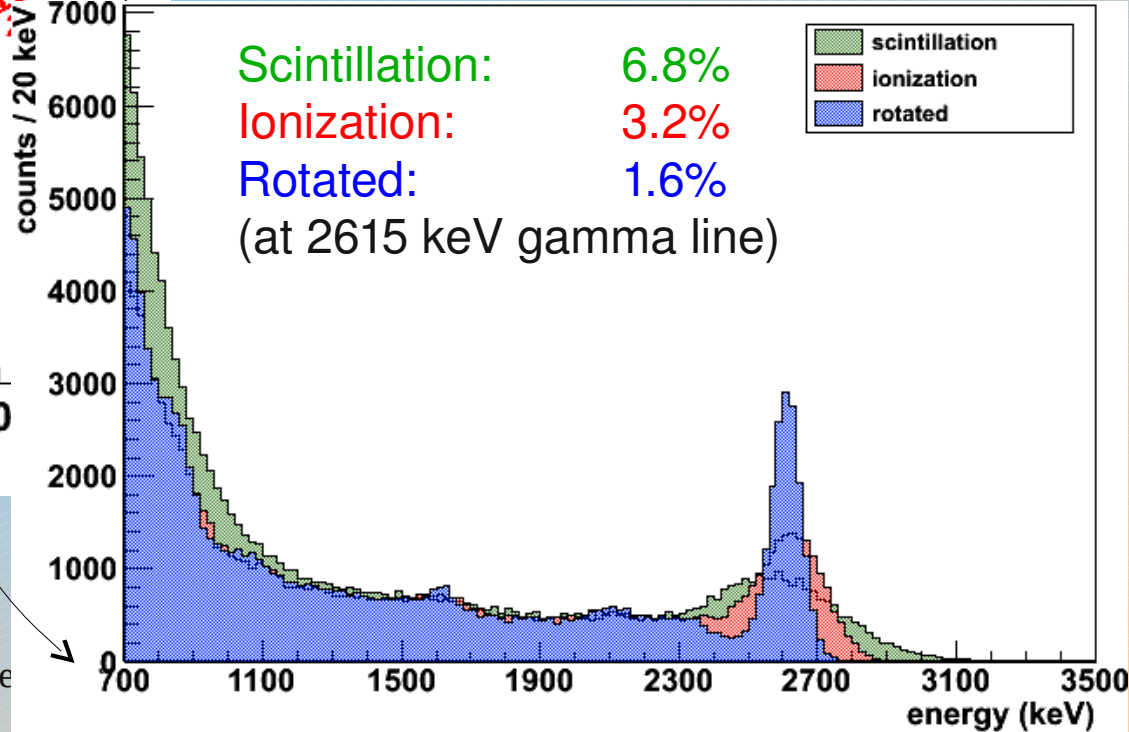
23.08.2013

V.Be

Properties of xenon cause increased scintillation to be associated with decreased ionization (and vice-versa)

E. Conti et al. Phys. Rev. B 68 (2003) 054201

Use projection onto a rotated axis to determine event energy

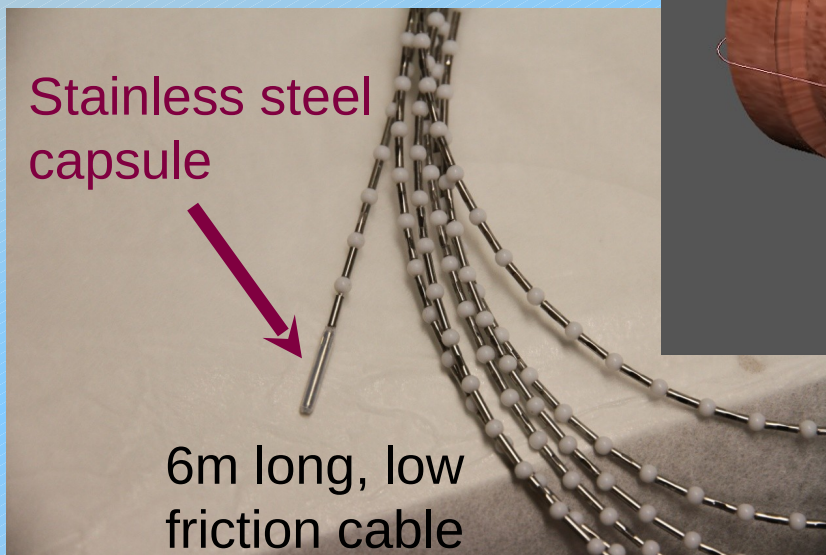
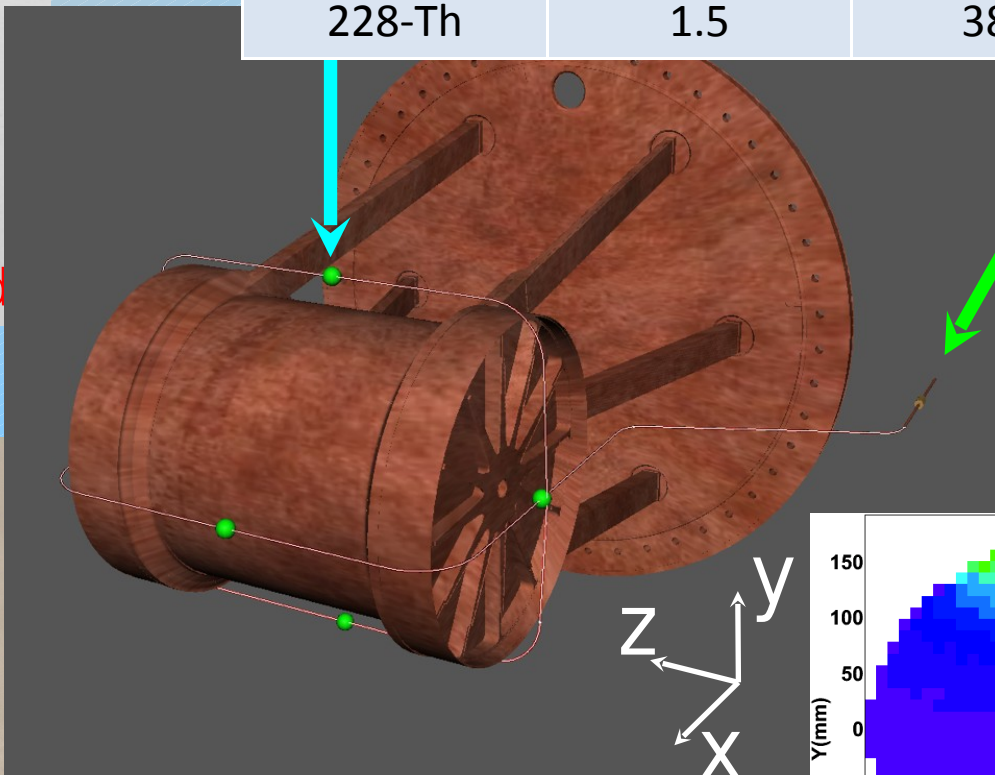


Calibrations

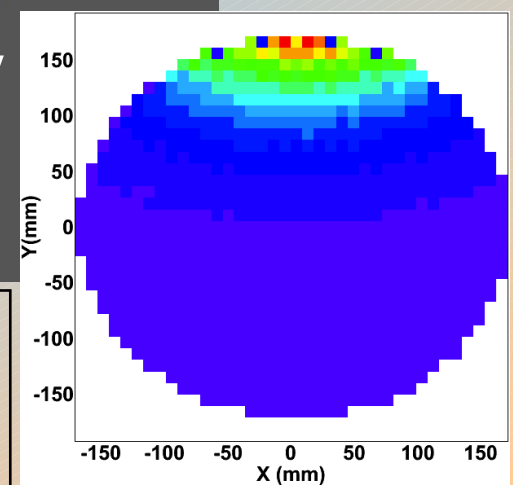
Miniaturized sources



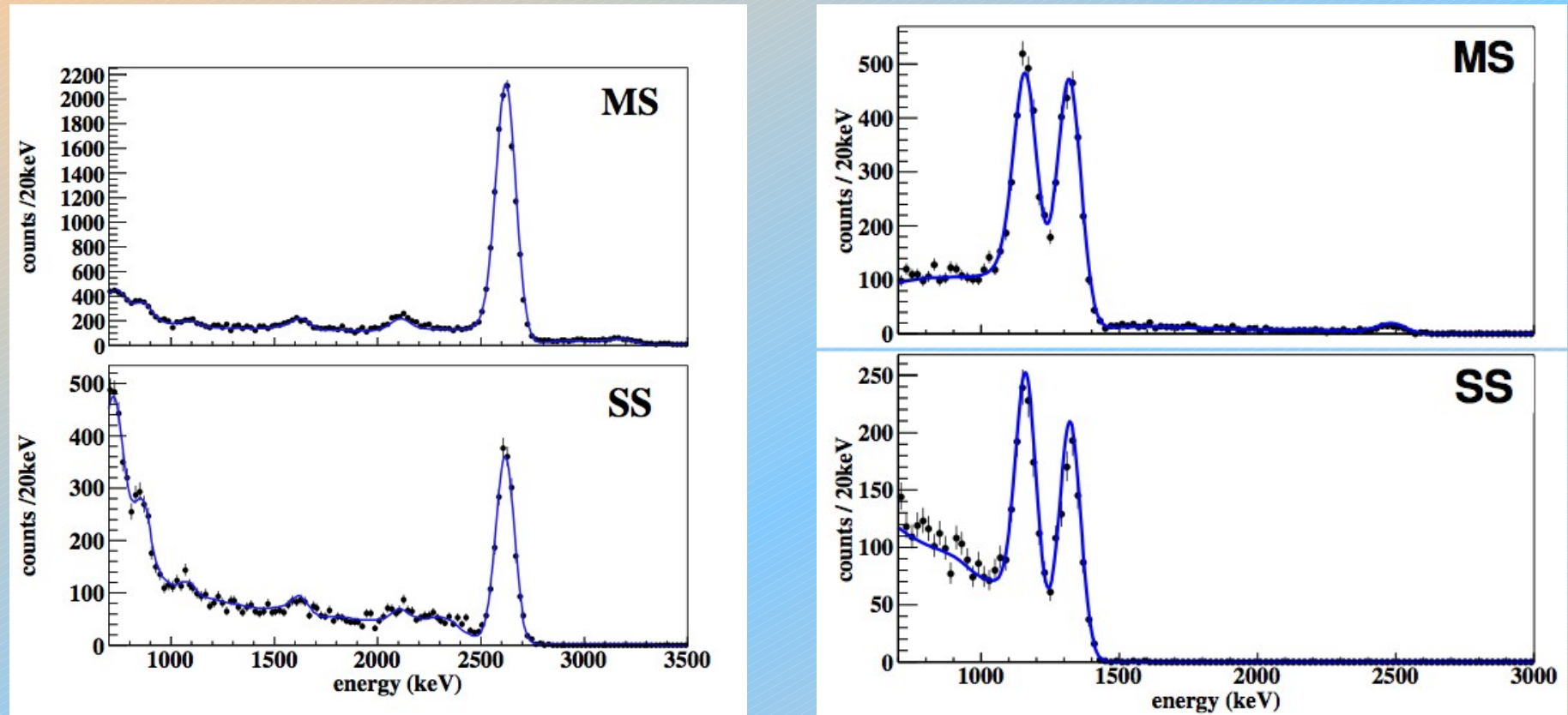
Source	Weak (kBq)	Strong (kBq)
60-Co	3.0	15.0
137-Cs	0.5	7.2
228-Th	1.5	38.0



Provide 4 full energy
deposition peaks in
the energy range
662 keV – 2615 keV

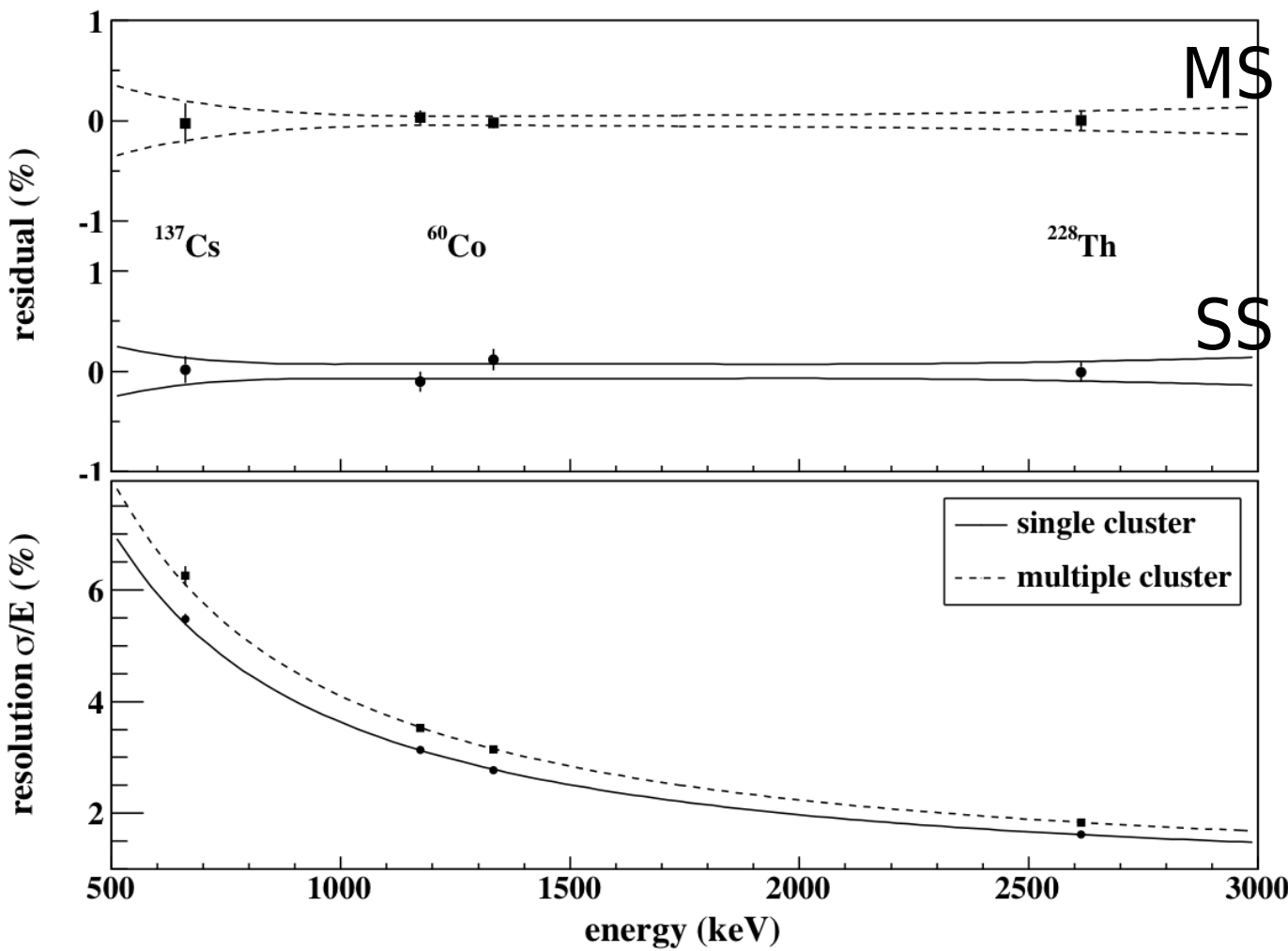


Calibrations source spectrum agreement



- Multi site (MS) and single site (SS) data (black points) are compared to model (blue curves)
- Single site fraction agrees to within 10%
- Can measure source activities better than 4%

Energy Calibration



Using quadratic model for energy calibration, single- and multi-site residual are < 0.1%

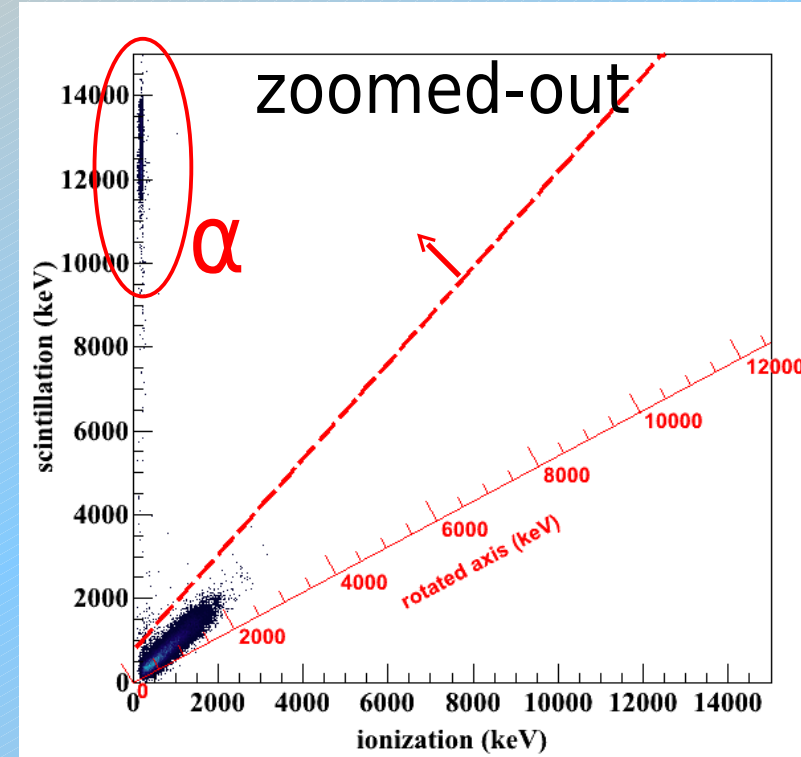
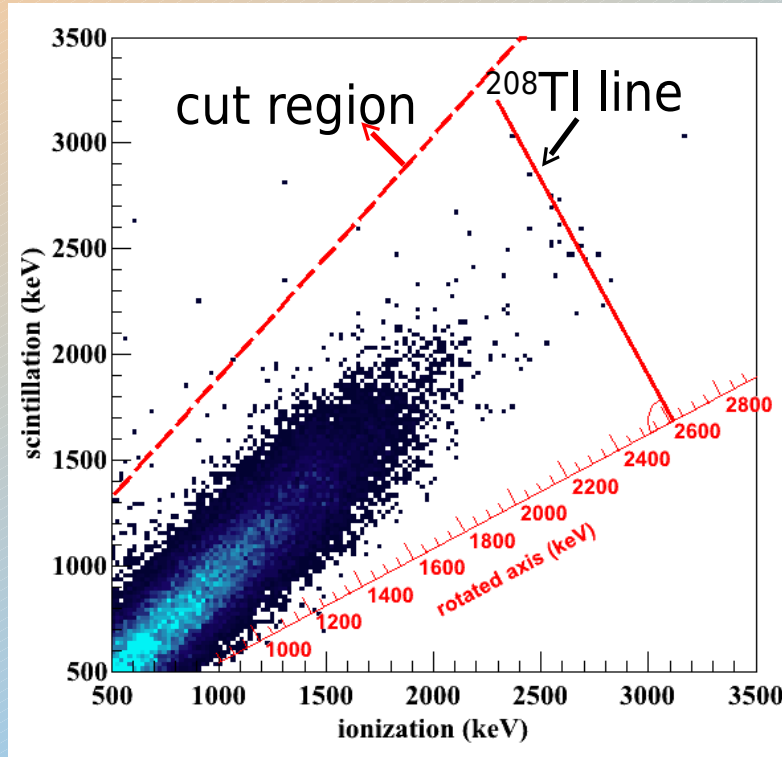
Energy resolution model:

$$\sigma_{Tot}^2 = p_0^2 E + p_1^2 + p_2^2 E^2$$

Resolution dominated by constant (noise) term p_1

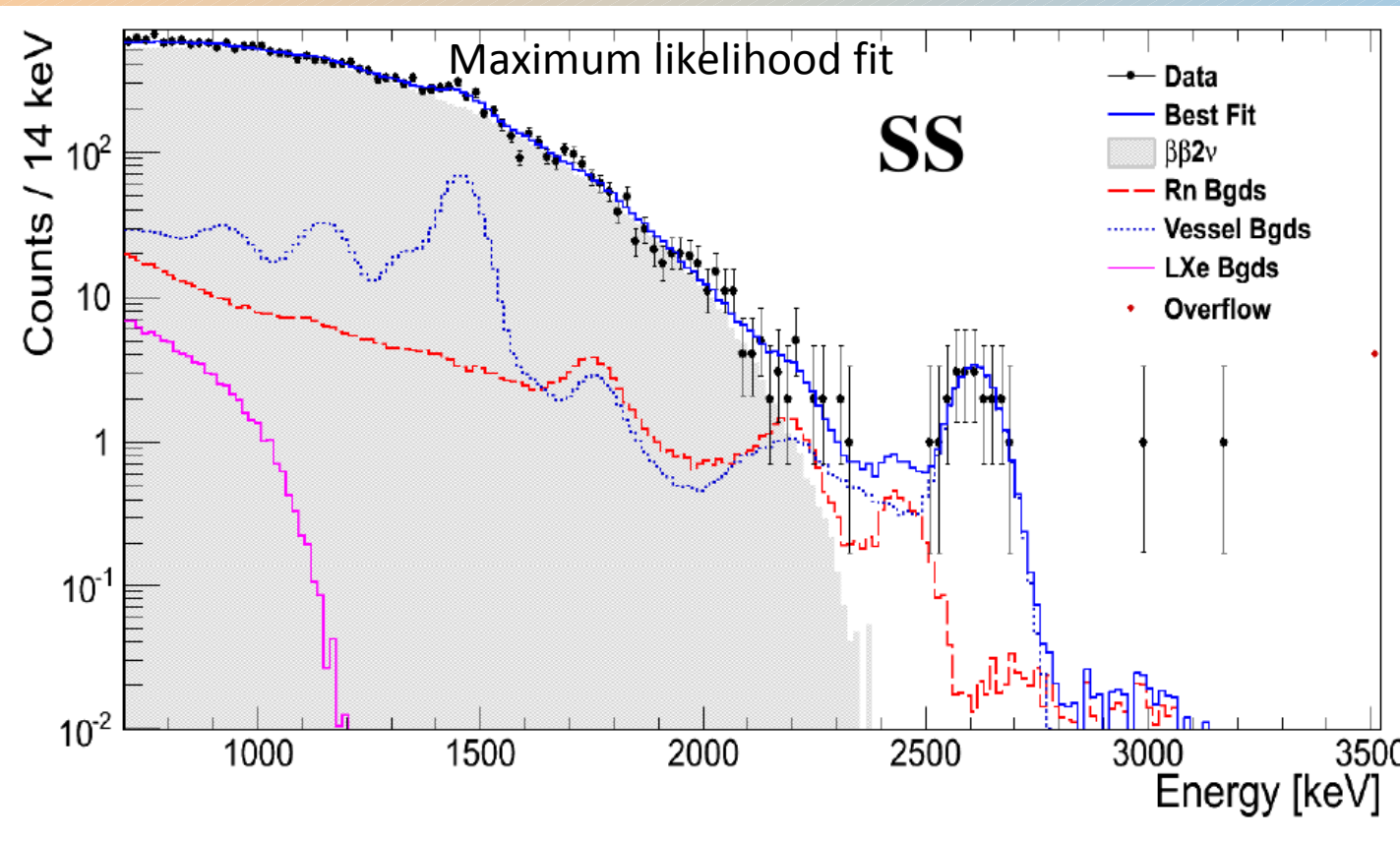
At $Q_{\beta\beta}$ (2458 keV):
 $\sigma/E = 1.84\%$ (SS)
 $\sigma/E = 1.93\%$ (MS)

Data analysis cuts



- Veto, noise, etc. anticoincidences (5.6% total dead-time)
- «Diagonal» cut to remove alphas and events with bad charge collection
- Only events with 1 scintillation and 3 coordinates reconstructed
- 700 keV low energy cut
- Fiducial cut (15 mm from cathode, 10 mm from anodes and 30 mm from teflon reflector)
- 58% efficiency for 2nu estimated by MC

Updated results for $2\beta 2\nu$



Trigger fully efficient above
700 keV

Low background run 2a
livetime: **127.6 days**
dead time: **5.6%**

Active mass:
82.75 kg LXe
(66.2 kg ^{136}Xe)

^{136}Xe exposure: **23.14 kg·yr**

Various background PDFs
fitted along with $2\nu\beta\beta$ and
 $0\nu\beta\beta$ PDFs

$$T_{1/2} = (2.172 \pm 0.017 \text{ stat} \pm 0.06 \text{ sys}) \cdot 10^{21} \text{ yr}$$

The most accurate $T_{1/2}$ of any $2\nu\beta\beta$ decay (arXiv:1306.6106)

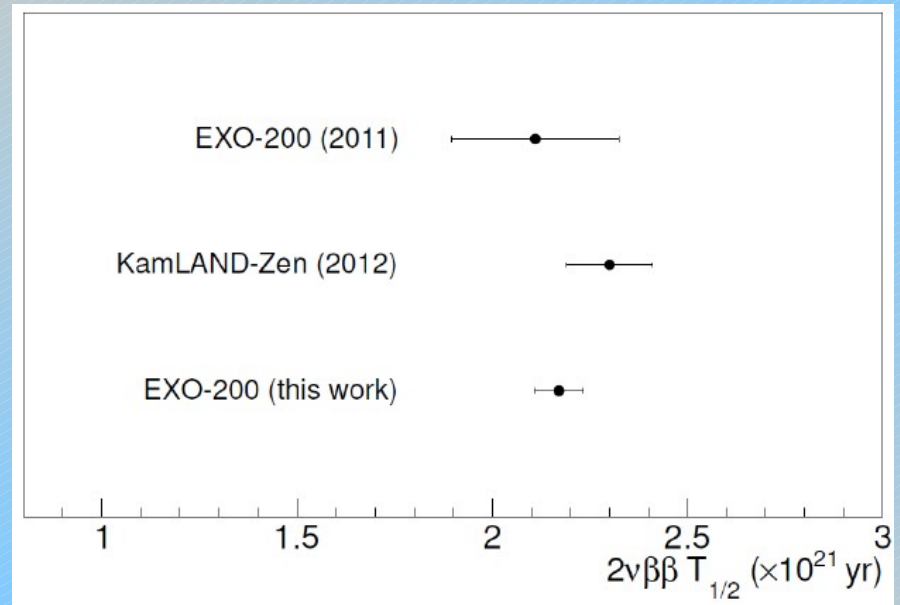
KamLAND-Zen

$$T_{1/2} = (2.38 \pm 0.02 \text{ stat} \pm 0.14 \text{ sys}) \cdot 10^{21} \text{ yr}$$

A.Gando et al., Phys. Rev. C 85 (2012) 045504

Comparison of the results for $2\beta 2\nu$

Comparison between
this result (improved Run 2a)
and EXO-200 (2011, Run 1)
and KamLAND-Zen (2012) results.

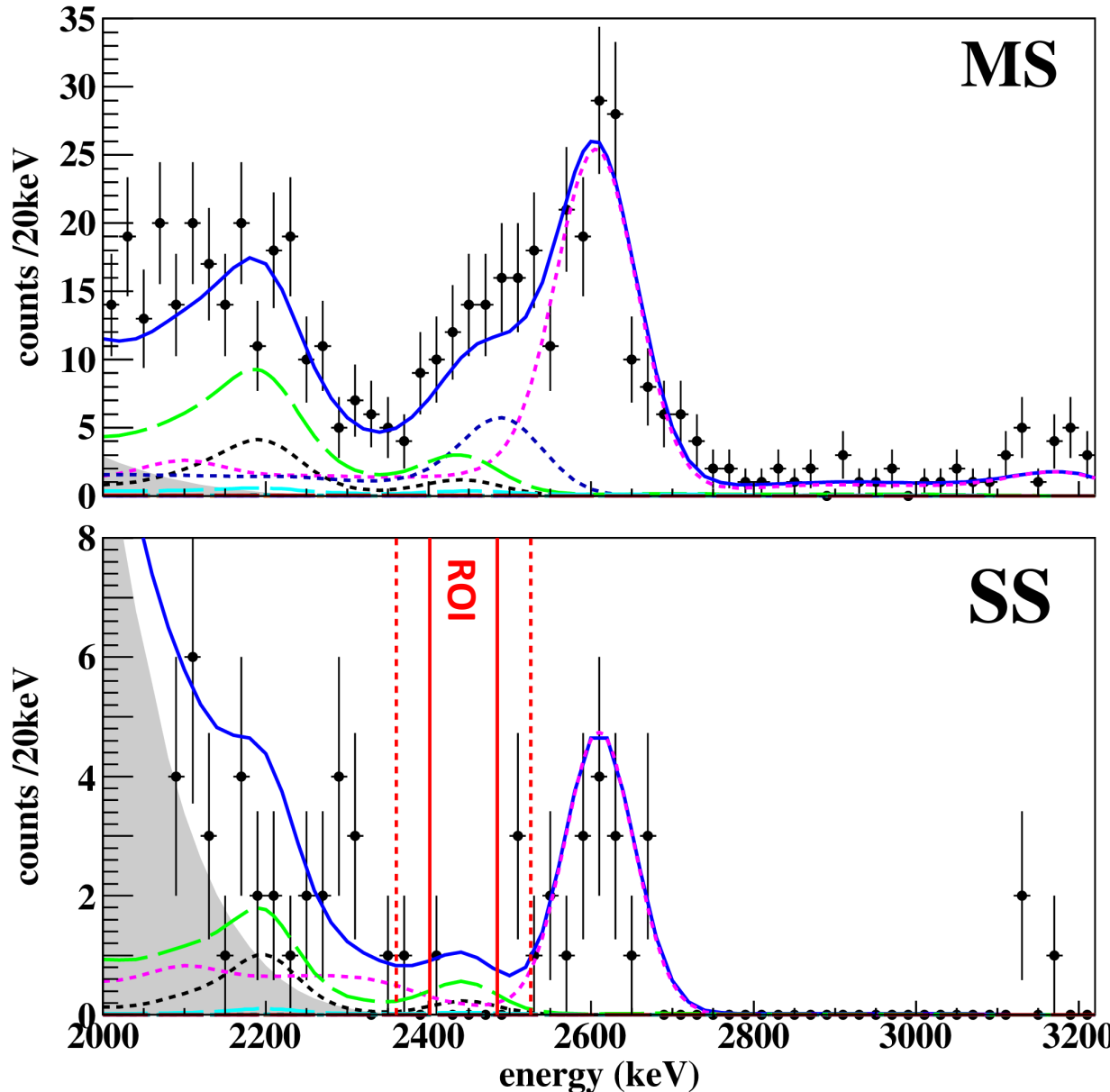


List of the most precise measurements of 2β . Only direct experiments shown.

Nuclide	$T_{1/2}^{2\nu\beta\beta} \pm \text{stat} \pm \text{sys}$ [y]	rel. uncert. [%]	$G^{2\nu}$ $[10^{-21} \text{ y}^{-1}]$	$M^{2\nu}$ $[\text{MeV}^{-1}]$	rel. uncert. [%]	Experiment (year)
^{136}Xe	$2.172 \pm 0.017 \pm 0.060 \cdot 10^{21}$	± 2.85	1433	0.0217	± 1.4	EXO-200 (this work)
^{76}Ge	$1.84^{+0.09+0.11}_{-0.08-0.06} \cdot 10^{21}$	$+7.7$ -5.4	48.17	0.129	$+3.9$ -2.8	GERDA (2013)
^{130}Te	$7.0 \pm 0.9 \pm 1.1 \cdot 10^{20}$	± 20.3	1529	0.0371	± 10.2	NEMO-3 (2011)
^{116}Cd	$2.8 \pm 0.1 \pm 0.3 \cdot 10^{19}$	± 11.3	2764	0.138	± 5.7	NEMO-3 (2010)
^{48}Ca	$4.4^{+0.5}_{-0.4} \pm 0.4 \cdot 10^{19}$	$+14.6$ -12.9	15550	0.0464	$+7.3$ -6.4	NEMO-3 (2010)
^{96}Zr	$2.35 \pm 0.14 \pm 0.16 \cdot 10^{19}$	± 9.1	6816	0.0959	± 4.5	NEMO-3 (2010)
^{150}Nd	$9.11^{+0.25}_{-0.22} \pm 0.63 \cdot 10^{18}$	$+7.4$ -7.3	36430	0.0666	$+3.7$ -3.7	NEMO-3 (2009)
^{100}Mo	$7.11 \pm 0.02 \pm 0.54 \cdot 10^{18}$	± 7.6	3308	0.250	± 3.8	NEMO-3 (2005)
^{82}Se	$9.6 \pm 0.3 \pm 1.0 \cdot 10^{19}$	± 10.9	1596	0.0980	± 5.4	NEMO-3 (2005)

Results for $2\beta 0\nu$

Zoomed around $0\nu\beta\beta$ region of interest (ROI)



Low background run 2a
No signal observed

Background in ± 1 ROI:
 $1.5 \cdot 10^{-3} \pm 0.1 \text{ kg}^{-1}\text{yr}^{-1}\text{keV}^{-1}$
- perfectly low

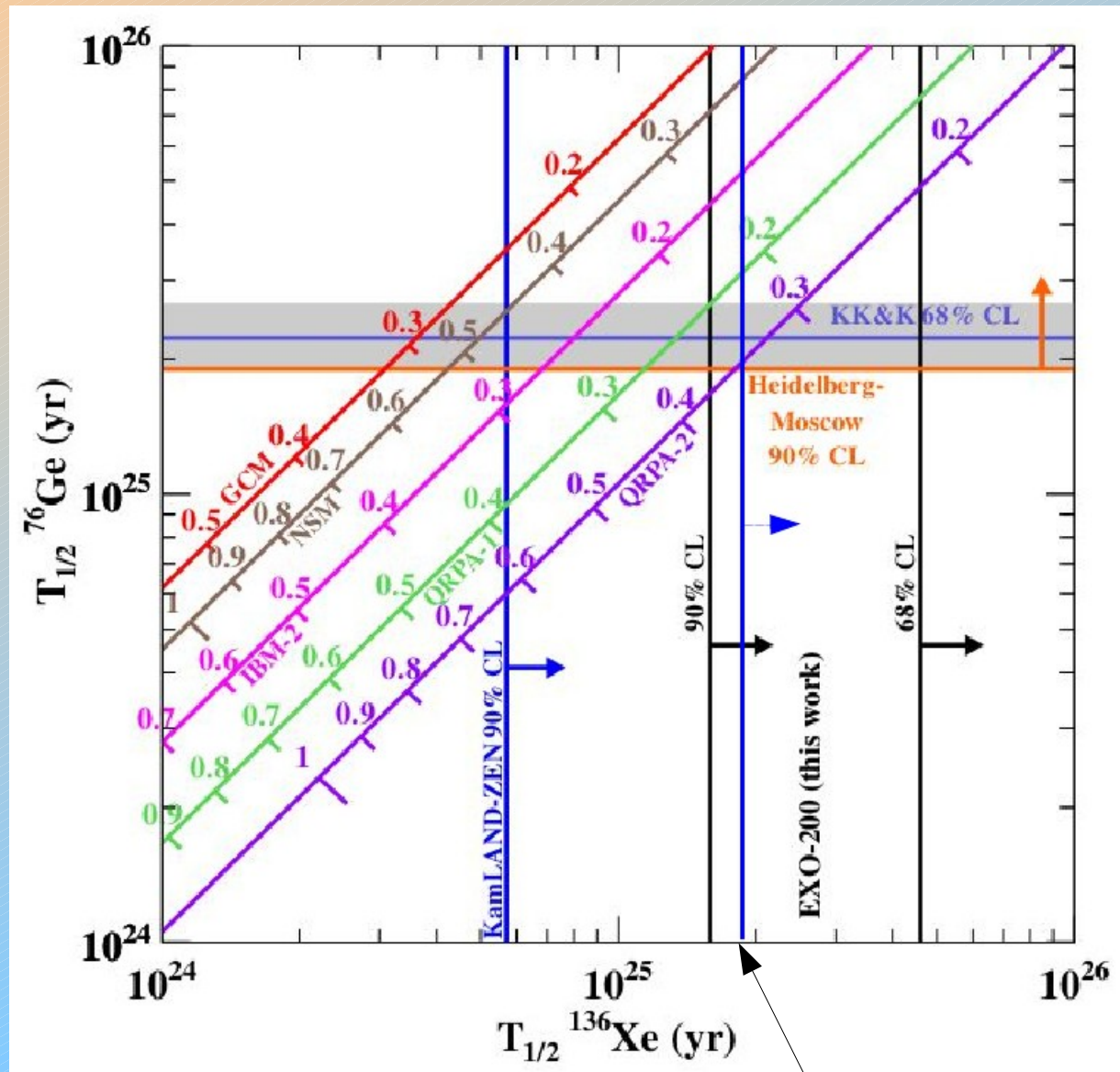
$T_{1/2}^{0\nu\beta\beta} ({}^{136}\text{Xe}) > 1.6 \cdot 10^{25} \text{ yr}$
(90% C.L.)

Phys. Rev. Lett. V.109 I.3 (2012)

Majorana mass limit
<140-380 meV

ββ2ν
ββ0ν (90% CL Limit)
⁴⁰K LXe Vessel
⁵⁴Mn LXe Vessel
⁶⁰Co LXe Vessel
⁶⁵Zn LXe Vessel
²³²Th LXe Vessel
²³⁸U LXe Vessel
¹³⁵Xe Active LXe
²²²Rn Active LXe
²²²Rn Inactive LXe
²¹⁴Bi Cathode Surface
²²²Rn Air Gap
.
Data
Total

Limits on $0\nu\beta\beta$



$T_{1/2}^{0\nu\beta\beta} ({}^{136}\text{Xe}) > 1.6 \cdot 10^{25} \text{ yr}$
 $\langle m_{\beta\beta} \rangle < 140\text{-}380 \text{ meV}$
 (90% C.L.)

EXO-200 contradicts Klapdor-Kleingrothaus and Krivosheina claim for $0\nu\beta\beta$ discovery at the 90% for most matrix elements

- A. Gando et al. Phys. Rev. C 85 (2012) 045504
 H.V. Klapdor-Kleingrothaus et.al. Eur. Phys. J. A12 (2001) 147
 H.V. Klapdor-Kleingrothaus and I.V. Krivosheina, Mod. Phys. Lett., A21 (2006) 1547.

Summary

EXO-200 is taking low background data,
approved at least end of 2014

About 3 times larger dataset acquired

Detector working well, met our goals:

Energy resolution: 1.84% at $Q_{\beta\beta}$

Background: $1.5 \times 10^{-3} \text{ kg}^{-1}\text{keV}^{-1}\text{yr}^{-1}$

1 (5) counts in 1σ (2σ) 0v $\beta\beta$ ROI

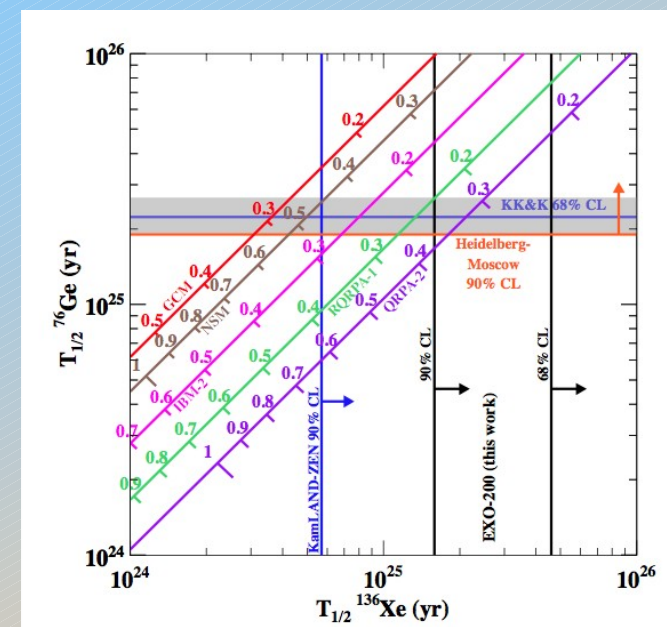
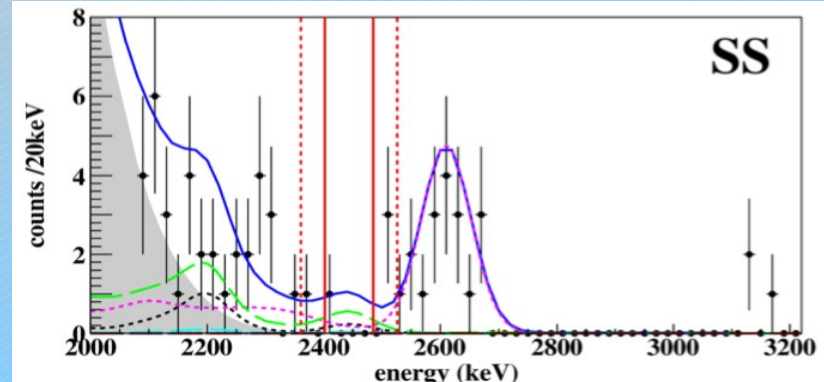
$$\begin{aligned} T_{1/2}^{0v\beta\beta} &> 1.6 \cdot 10^{25} \text{ yr} \\ \langle m_{\beta\beta} \rangle &< 140-380 \text{ meV} \\ &\text{(90\% C.L.)} \end{aligned}$$

Phys. Rev. Lett. V.109 I.3 (2012)

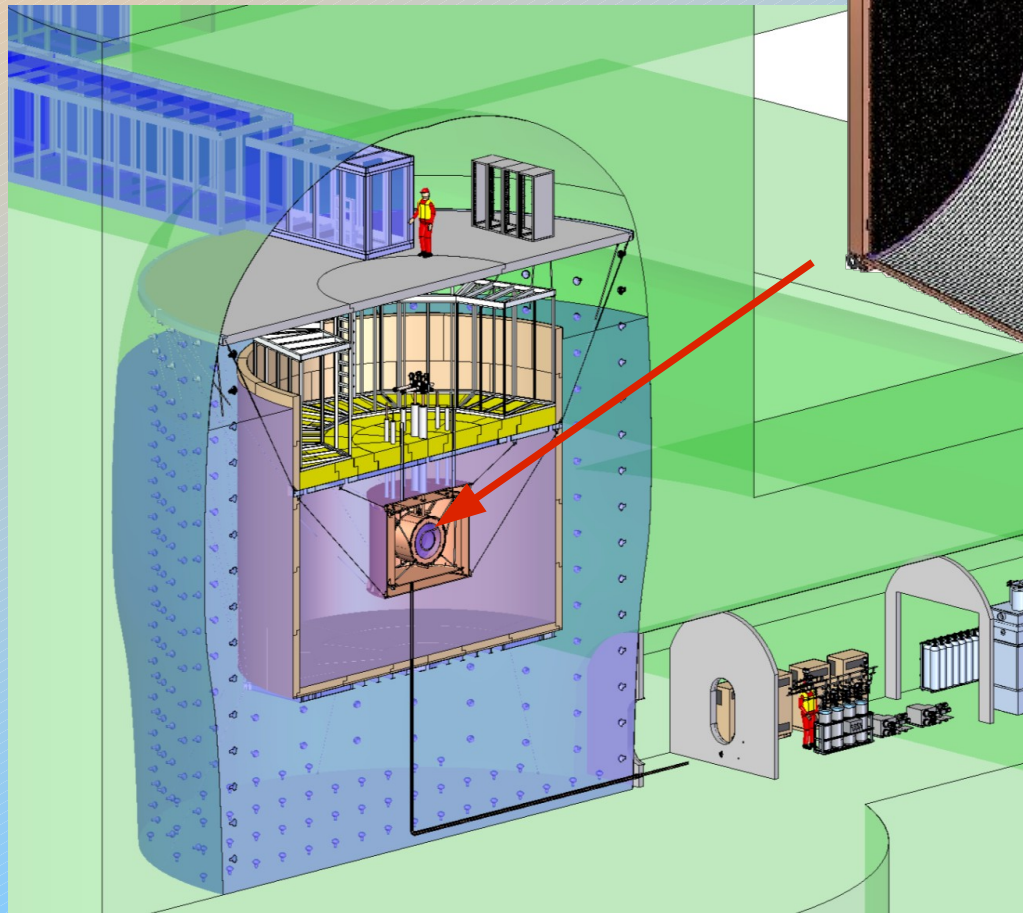
R&D for the next generation (nEXO) started

23.08.2013

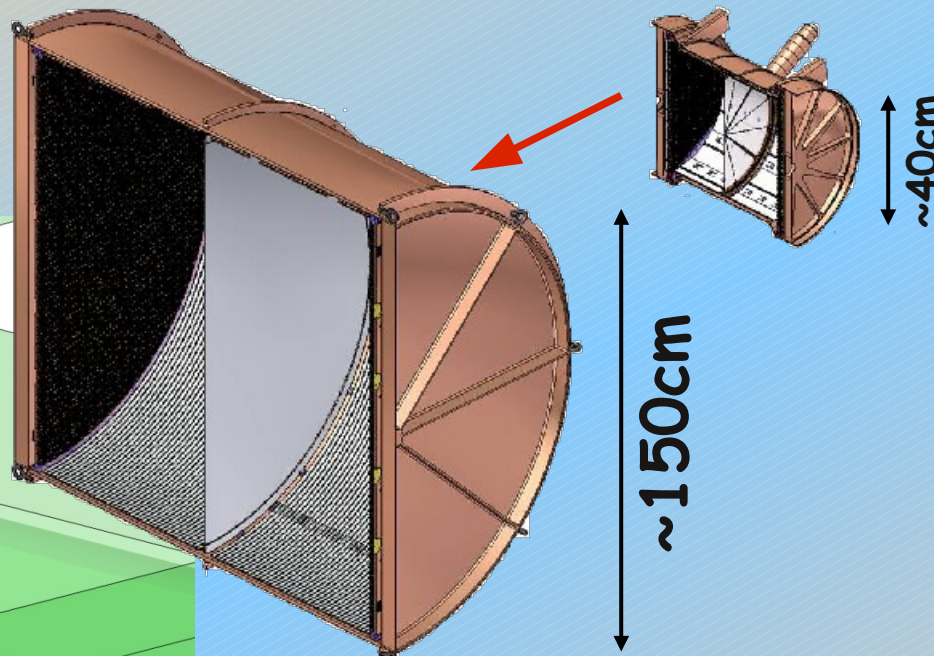
V.Belov EXO-200



nEXO at SNOLab

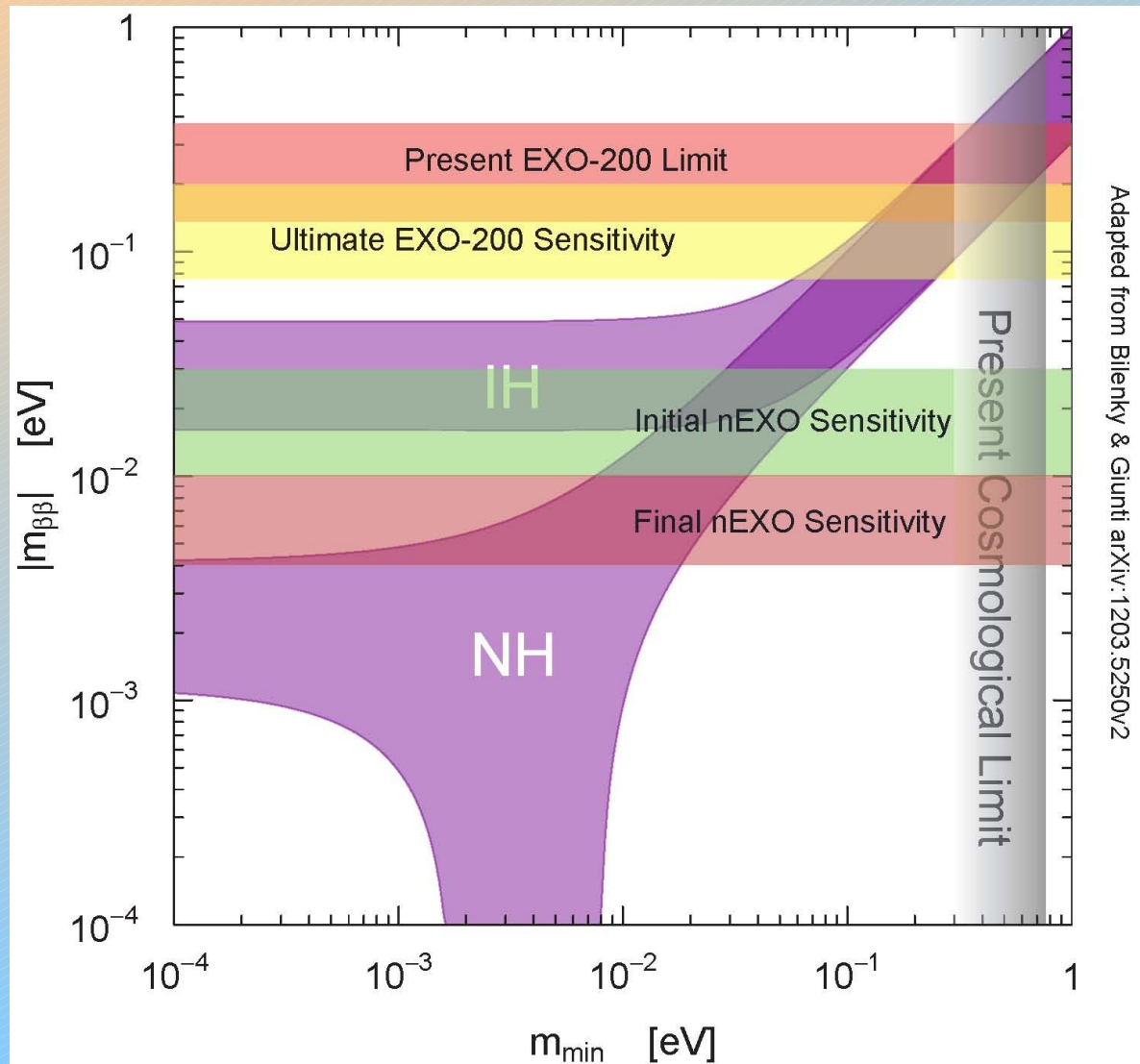


Conceptual design for SNOLab



- 5 tonne LXe TPC “as similar to EXO200 as possible”
- R&D for cold electronics, SiPM photodetectors, alternative charge collection scheme
- Provide access ports for a possible later upgrade to Ba tagging

EXO-200 and nEXO projected sensitivities



Blue bands are 68%CL from oscillation experiments for "Inverted" and "Normal" Hierarchy

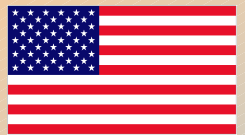
The EXO-200 "Present limit" is the 90%CL envelope of Limits (for different NMEs) from PRL 109 (2012) 032505

The EXO-200 "Ultimate" sensitivity: 90%CL for no signal in 4 yrs livetime with new analysis & Rn removal

The "Initial nEXO" band refers to a detector directly scaled from EXO-200, including its measured background and 10yr livetime.

The "Final nEXO" band refers to the same detector and no background other than 2ν

The EXO Collaboration



University of Alabama, Tuscaloosa AL, USA - D. Auty, T. Didberidze, M. Hughes, A. Piepke, K. Pushkin, M. Volk

University of Bern, Switzerland - M. Auger, S. Delaquis, D. Franco, G. Giroux, R. Gornea, T. Tolba, J-L. Vuilleumier, M. Weber

California Institute of Technology, Pasadena CA, USA - P. Vogel

Carleton University, Ottawa ON, Canada - M. Dunford, K. Graham, C. Hargrove, R. Killick, F. Leonard, C. Licciardi, C. Oullet, D. Sinclair, V. Strickland

Colorado State University, Fort Collins CO, USA - C. Benitez-Medina, C. Chambers, A. Craycraft, W. Fairbank, Jr., N. Kaufhold, T. Walton

Drexel University, Philadelphia PA, USA - M.J. Dolinski, M.J. Jewell, Y.H. Lin, E. Smith

University of Illinois, Urbana-Champaign IL, USA - D. Beck, J. Walton, M. Tarka, L. Yang

IHEP Beijing, People's Republic of China - G. Cao, X. Jiang, Y. Zhao

Indiana University, Bloomington IN, USA - J. Albert, S. Daugherty, T. Johnson, L.J. Kaufman

University of California, Irvine, Irvine CA, USA - M. Moe

ITEP Moscow, Russia - D. Akimov, I. Alexandrov, V. Belov, A. Burenkov, M. Danilov, A. Dolgolenko, A. Karelin, A. Kovalenko, A. Kuchenkov, V. Stekhanov, O. Zeldovich

Laurentian University, Sudbury ON, Canada - E. Beauchamp, D. Chauhan, B. Cleveland, J. Farine, B. Mong, U. Wichoski

University of Maryland, College Park MD, USA - C. Davis, A. Dobi, C. Hall, S. Slutsky, Y-R. Yen

University of Massachusetts, Amherst MA, USA - T. Daniels, S. Johnston, K. Kumar, M. Lodato, C. Mackeen, K. Malone, A. Pocar, J.D. Wright

University of Seoul, South Korea - D. Leonard

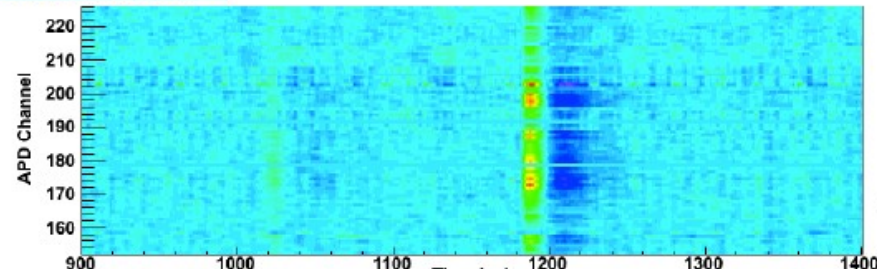
SLAC National Accelerator Laboratory, Menlo Park CA, USA - M. Breidenbach, R. Conley, K. Fouts, R. Herbst, S. Herrin, A. Johnson, R. MacLellan, A. Odian, C.Y. Prescott, P.C. Rowson, J.J. Russell, K. Skarpaas, M. Swift, A. Waite, M. Wittgen, J. Wodin

Stanford University, Stanford CA, USA - P.S. Barbeau, J. Bonatt, T. Brunner, J. Chaves, J. Davis, R. DeVoe, D. Fudenberg, G. Gratta, S. Kravitz, D. Moore, I. Ostrovskiy, K. O'Sullivan, A. Rivas, A. Sabourov, A. Schubert, D. Tosi, K. Twelker, L. Wen

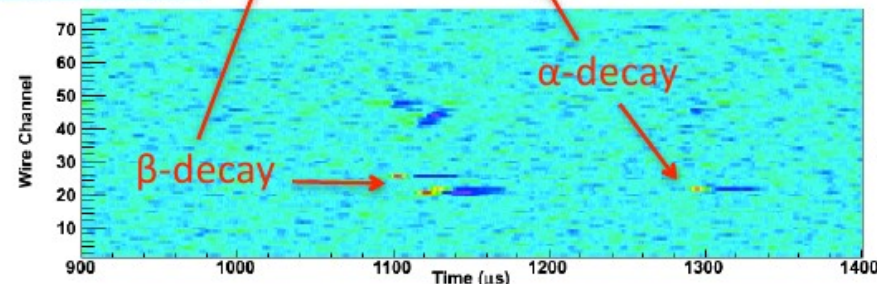
Technical University of Munich, Garching, Germany - W. Feldmeier, P. Fierlinger, M. Marino

Rn Content in Xenon

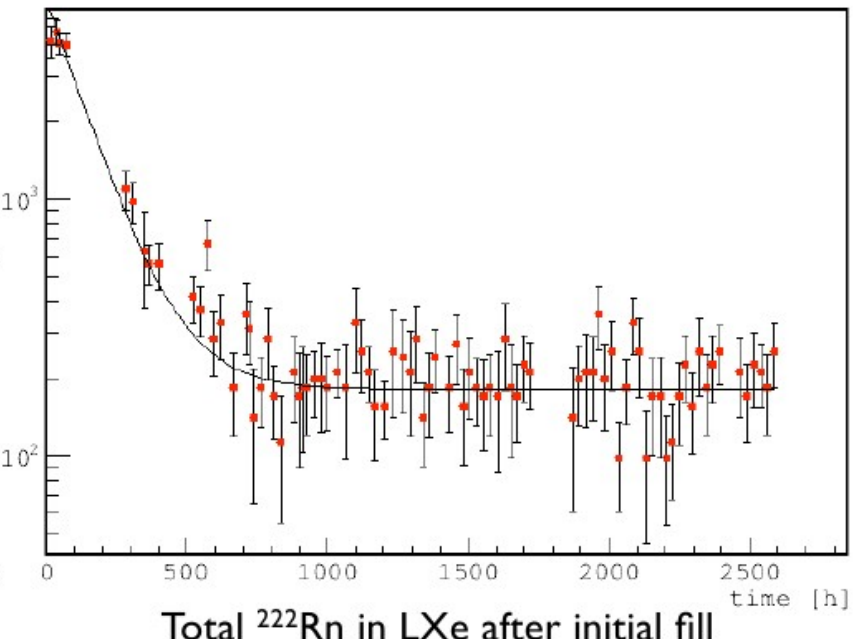
Scintillation



Ionization



$^{214}\text{Bi} - ^{214}\text{Po}$ correlations in the EXO-200 detector

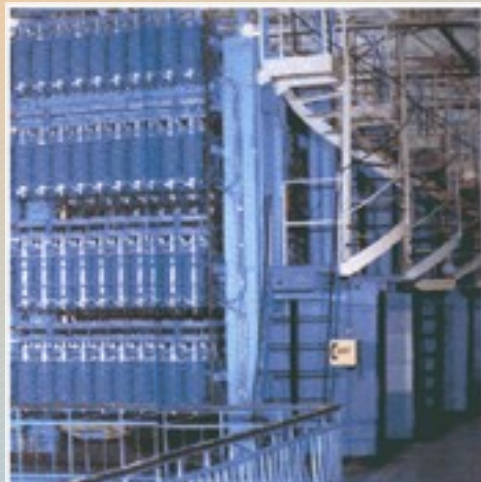


Total ^{222}Rn in LXe after initial fill

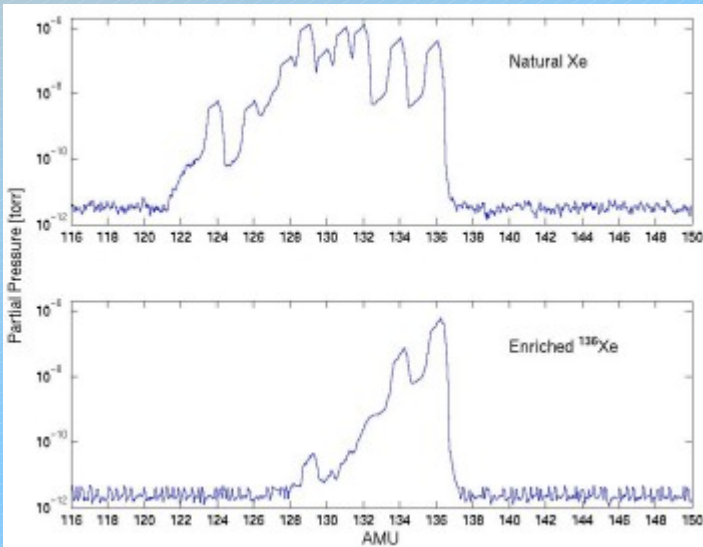
Using the Bi-Po (Rn daughter) coincidence technique, we can estimate the Rn content in our detector. The ^{214}Bi decay rate is consistent with measurements from alpha-spectroscopy.

Long-term study shows a constant source of ^{222}Rn dissolving in ${}^{\text{enr}}\text{LXe}$: $360 \pm 65 \mu\text{Bq}$ (Fid. vol.)

EXO-200: the first 200kg Double Beta Decay Experiment



Centrifuge facility in Russia



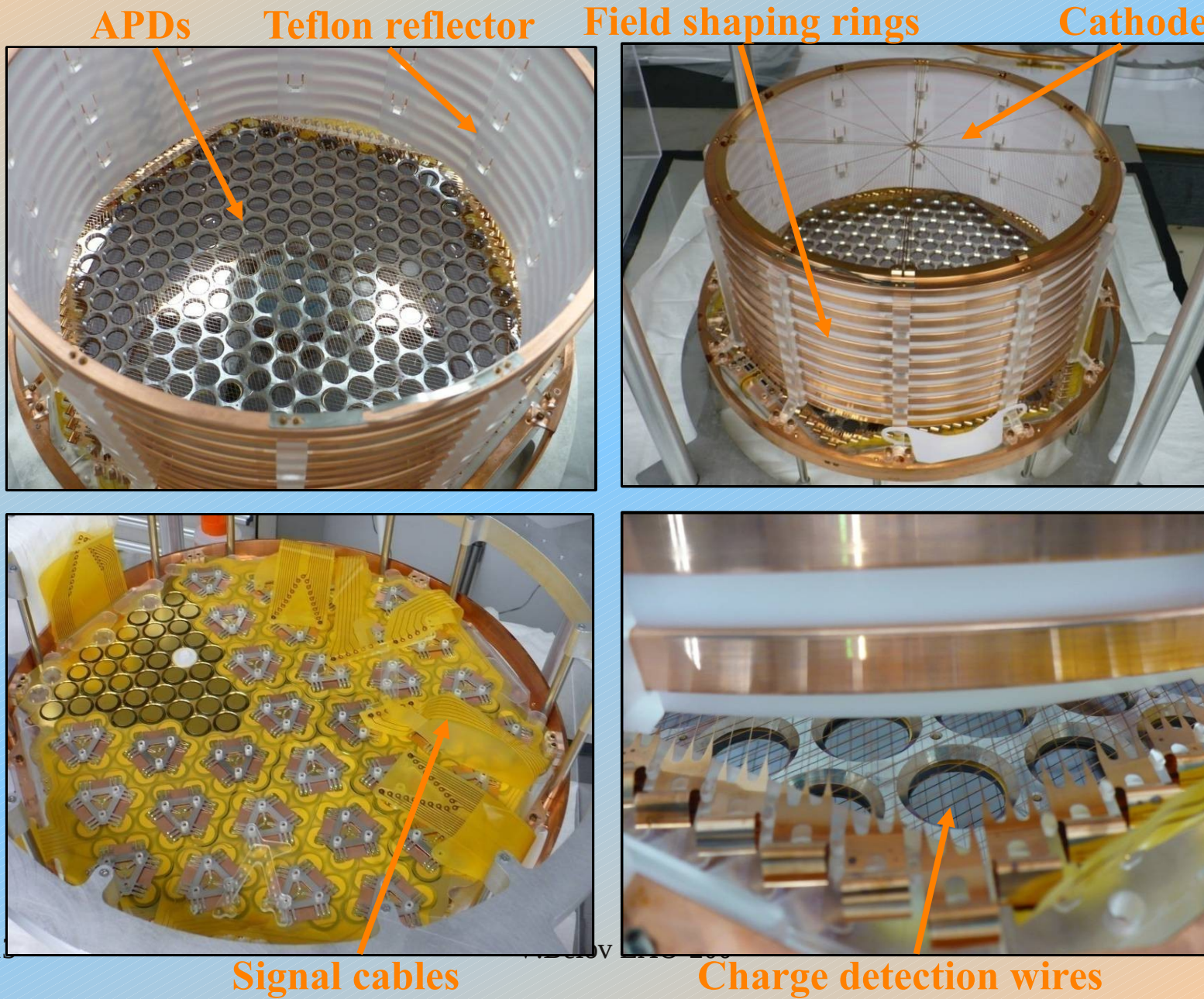
RGA mass scan of xenon samples
23.08.2013



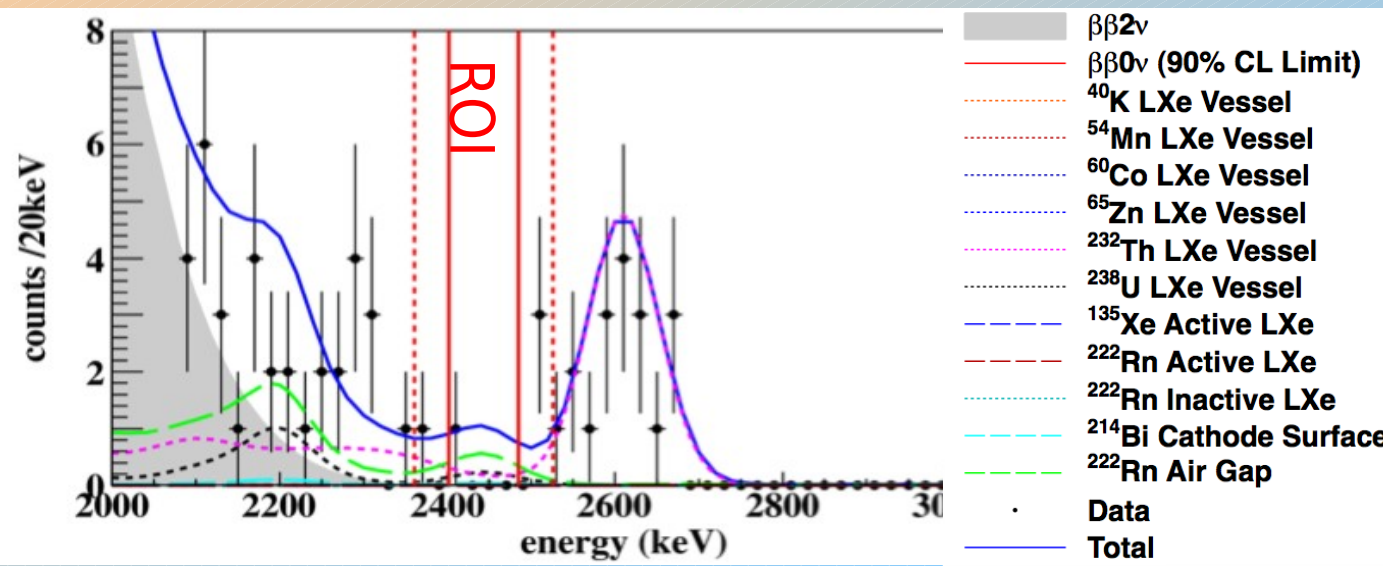
Enriched xenon storage bottles for EXO

EXO collaboration currently have
200 kg of xenon enriched to 80% =
160 kg of ^{136}Xe

The EXO-200 TPC



Background counts in $\pm 1,2 \sigma$ ROI



EXO-200 goal
(slide 3):

40 cnts/2y in $\pm 2\sigma$
ROI,
140 kg LXe

In this data 120
days, 98.5 kg, this
would be: 4.6

	Expected events from fit			
	$\pm 1 \sigma$	$\pm 2 \sigma$	$\pm 1 \sigma$	$\pm 2 \sigma$
^{222}Rn in cryostat air-gap	1.9	± 0.2	2.9	± 0.3
^{238}U in LXe Vessel	0.9	± 0.2	1.3	± 0.3
^{232}Th in LXe Vessel	0.9	± 0.1	2.9	± 0.3
^{214}Bi on Cathode	0.2	± 0.01	0.3	± 0.02
All Others	~ 0.2		~ 0.2	
Total	4.1	± 0.3	7.5	± 0.5
Observed	1		5	
Background index b ($\text{kg}^{-1}\text{yr}^{-1}\text{keV}^{-1}$)	$1.5 \cdot 10^{-3} \pm 0.1$		$1.4 \cdot 10^{-3} \pm 0.1$	

Expected from the
fit: 7.5

Observed: 5

Background
within
expectation

KamLand-ZEN

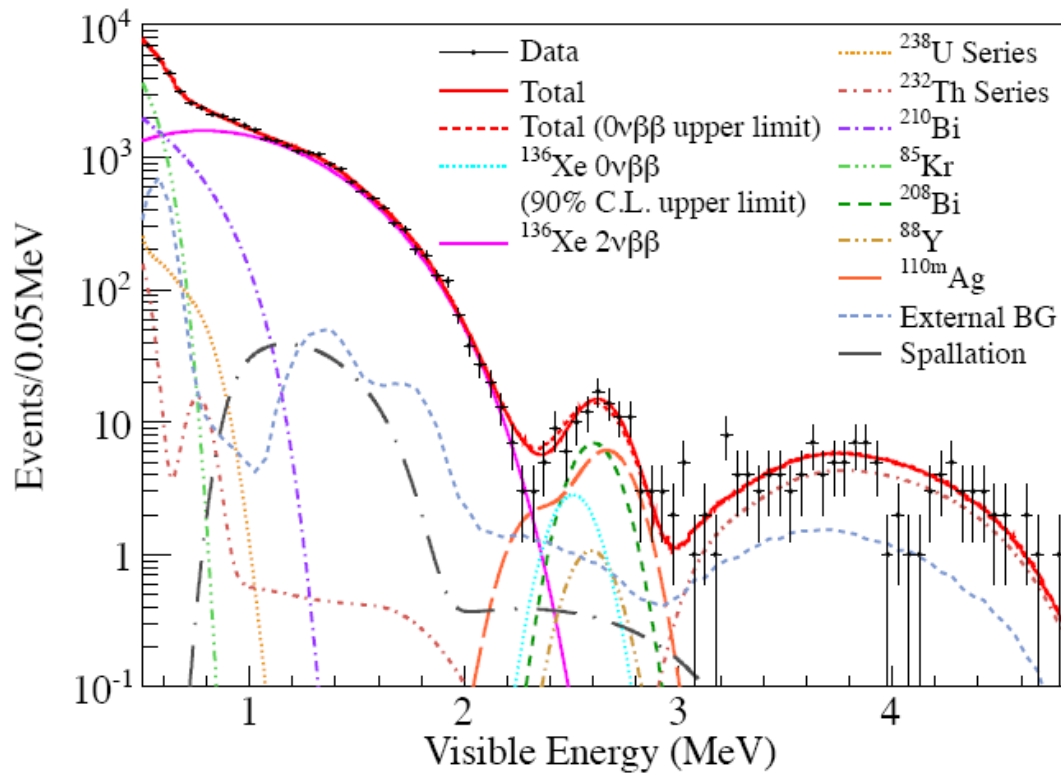


FIG. 4: Energy spectrum of selected $\beta\beta$ decay candidates together with the best-fit backgrounds and $2\nu\beta\beta$ decays, and the 90% C.L. upper limit for $0\nu\beta\beta$ decays.

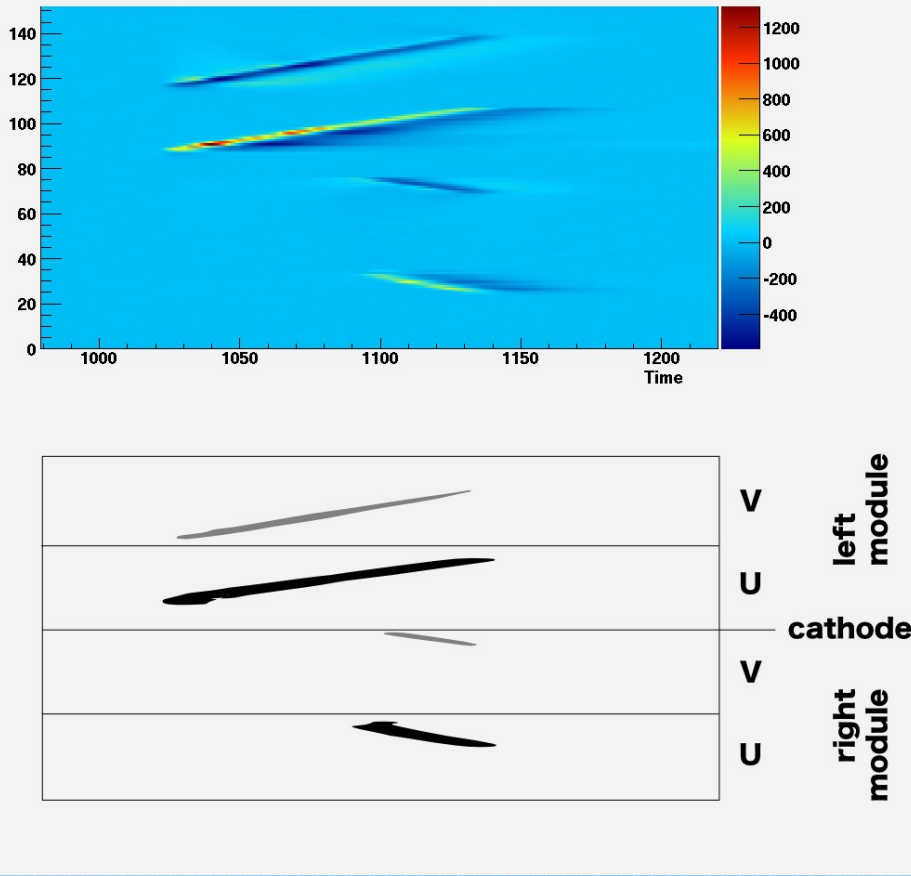
112.3 days 38.6kg-yr

$T_{2\nu}^{1/2} = 2.30 \pm 0.02(\text{stat}) \pm 0.12(\text{syst}) \times 10^{21}$ years arXiv:1205.6372

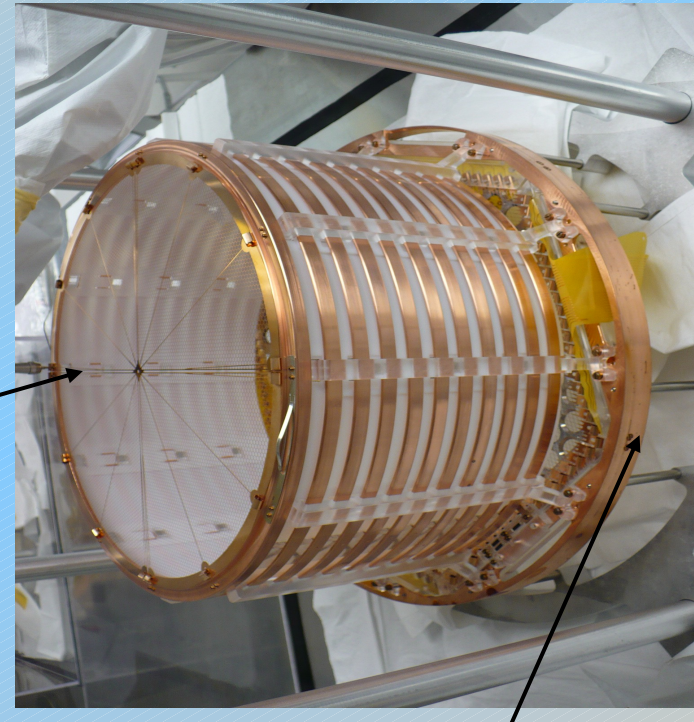
$T_{0\nu}^{1/2} > 6.2 \times 10^{24}$ years (KL-Zen 112days)

23.08.2013 $\langle m_{\beta\beta} \rangle < 0.26 \sim 0.54$ eV @90% C.L. V.Belov EXO-200

Muon track in EXO-200



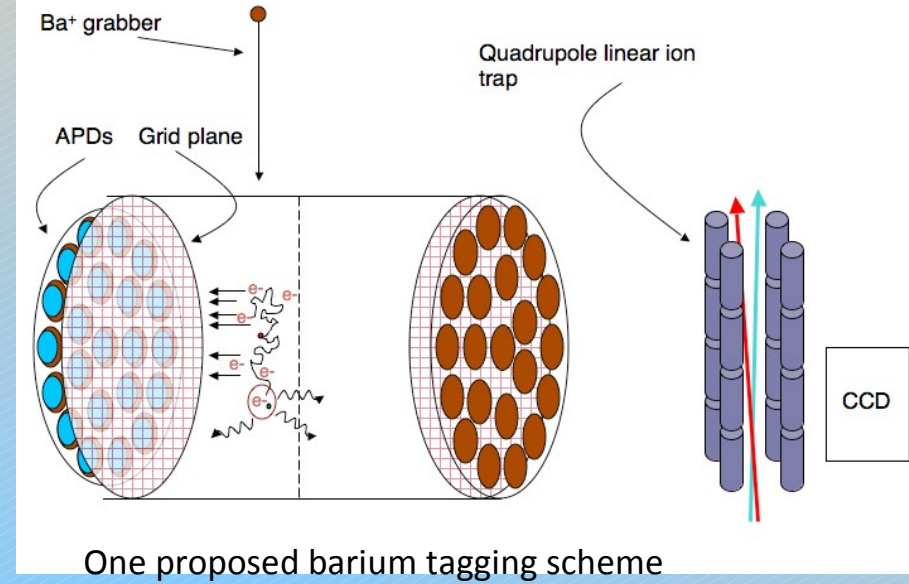
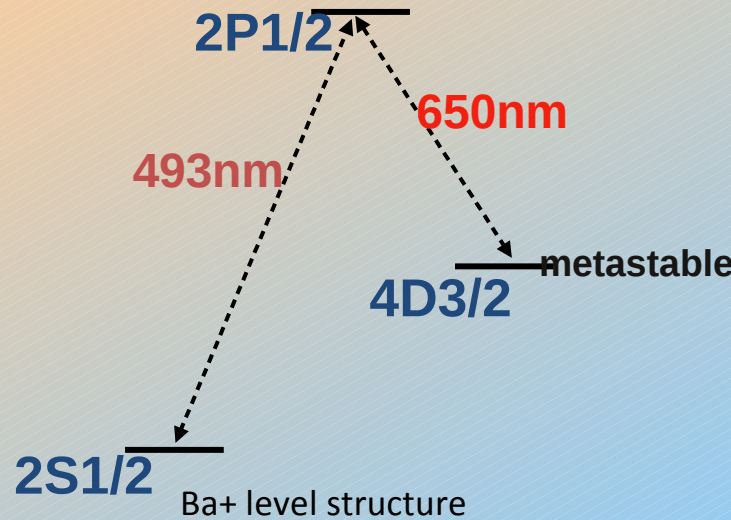
One of the two TPC modules



U and V wires

A track from a cosmic-ray muon in EXO-200. The horizontal axis represents time (uncalibrated for now) while the vertical is the wire position (see sketch). V wires see inductive signals while U wires collects the charge.
The muon in the present event traverses the cathode grid, leaving a long track in one TPC module and a shorter one in the other.

Barium Tagging R&D Summary



Method	Summary
RIS probe	Desorb and resonantly ionize Ba from probe tip, then identify with laser spectroscopy in ion trap
Hot probe	Release neutral by heating and ionize with hot surface, then identify with laser spectroscopy in ion trap
Solid Xe probe	Storage and spectroscopy of Ba ⁺ in Xe ice
Direct tag in liquid	Laser identification of Ba ⁺ in liquid Xe
Gas Xe extraction	Guide ions from high pressure (10 bar) Xe to low pressure trapping region, then identify with laser spectroscopy